Investigation of low-latitude ionospheric F region irregularities during the geomagnetic storm of 7-8 September 2017

Han Jin[1,2], Shasha Zou[2], Gang Chen[1]

[1]Electronic Information School, Wuhan University, Wuhan, China

[2]Department of Climate and Space Sciences and Engineering, University of Michigan, MI, USA

1 Introduction

- The low-latitude F region field-aligned irregularities (FAIs) may cause rapid variations in phase and amplitude of radio signals and lead to detrimental effect on navigation and communication system. Therefore, it is important to understand the underlying generation mechanism of these ionospheric irregular structures.
- It has been generally accepted that FAIs are mainly generated via the generalized Rayleigh-Taylor (RT) instability that may develop at the bottomside of the F layer and rapidly arise to the topside ionosphere.
- The low-latitude FAIs usually occur during postsunset hours due to the evening pre-reversal enhancement (PRE) of zonal electric field, which provides favorable conditions for the growth of the RT instability by lifting the lower F layer to higher altitudes where the ion-neutral collision frequency is lower.
- The PRE of zonal electric field is one of the most important factors for facilitating quiet time FAIs generation, but during storm time, other factors can also lead to perturbation in zonal electric field and thus facilitate the generation of FAIs.
- Under geomagnetic disturbance conditions, the low-latitude zonal electric field can be modified by two important drivers, i.e., prompt penetration of electric field (PPEF) and disturbance dynamo electric field (DDEF) driven by disturbed global thermospheric circulation.
- The suppression or initiation of the FAIs during the geomagnetic storm largely hinges on the competitive effects of these perturbation electric fields.
- In this study, we investigate the development of the low-latitude FAIs during the 7–8 September 2017 storm.

2 Instruments

Hainan Coherent Scatter Phased Array Radar

1. 7-beam (east-west plane) VHF radar operated at Fuke, Hainan Island, China.
2. It operates at 47 MHz with 54-kW peak power and 2-MHz bandwidth to detect the 3.2-m-scale FAIs.
3. Beam 4 of the radar points to the geographic north.
4. The central direction of the 7 radar beams is almost perpendicular to the local geomagnetic field at ionospheric E and F region altitudes to ensure the simultaneous observations of E and F region FAIs.

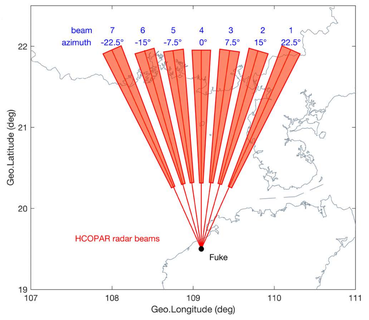

Figure 1. Map projection of the seven beam directions of Hainan Coherent Scatter Phased Array Radar (HCOPAR).

Hainan Digisonde

1. The background ionospheric condition and drifts are recorded by a co-located Digisonde.
2. The virtual height of the bottomside F layer, h'F, can be manually scaled from an ionogram. The mean vertical and zonal drift velocities in the F region can be calculated from Doppler skymap according to the angle of arrival and Doppler velocity of the echoes.

3 Observations

IMF and Solar Wind during 7–8 Sep 2017 storm

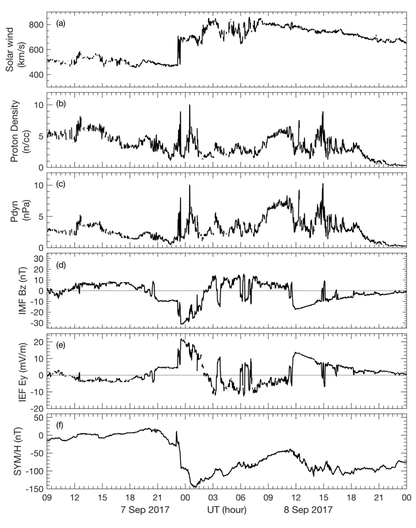

Figure 2. Temporal variations of (a) solar wind velocity (km/s), (b) solar wind density (n/cm^3), (c) solar wind dynamic pressure (nPa), (d) IMF Bz (nT), (e) IEF Ey (mV/m), and (f) SYM/H index (nT) during 7–8 September 2017.

First main phase:

- Commenced at ~23:31 UT on Sep 7 2017 with a steep IMF Bz southward excursion to -31.2 nT and the IEF Ey component reached ~21 mV/m.
- The IMF Bz remained southward for more than 2 hr, became northward at ~02:30 UT on Sep 8 and remained northward for ~9 hr.

Second Main phase:

- Another large and rapid IMF Bz southward turning occurred at 11:55 UT on Sep 8 , reaching ~-17.4 nT and the IEF Ey component reached ~13.76 mV/m.

Hainan Digisonde Observations

a) Postsunset F layer uplift:

- h'F uplifted significantly by 150 km right after the second IMF Bz southward turning, and reached a peak height of 387 km at ~12:35 UT.

b) Postmidnight F layer uplift:

- h'F again started to increase after 17:00 UT and reached a peak height of ~390km.

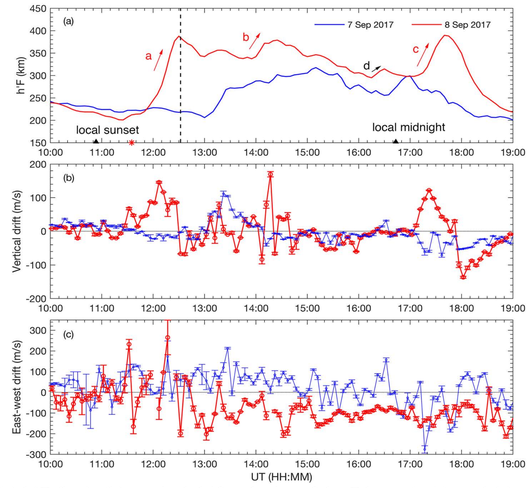

Figure 3. (a) h'F (km), (b) vertical drift velocity of the F layer (m/s), and (c) zonal drift of the F layer (m/s). The red asterisk indicates the time when IEF Ey suddenly turned eastward. The vertical dashed line indicates the initial time of the FAIs observed by the HCOPAR. Error bars represent the velocity spread.

c) Background plasma zonal drift:

Sep 8, 2017

- The velocity was almost westward, varying from about -16 to -200 m/s after ~12:45 UT, before which the zonal drift fluctuated between eastward and westward.

Sep 7, 2017:

- The nighttime zonal drift of the background plasma was mostly eastward.

Ionospheric Irregularities During the Storm

Multi-beam observation

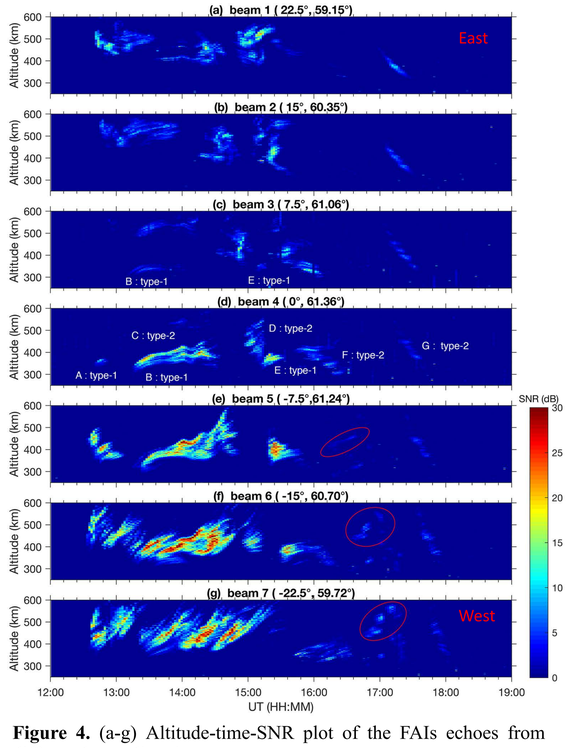

Figure 4. (a-g) Altitude-time-SNR plot of the FAIs echoes from different beam directions.

Type 1 echoes

- Freshly generated within the field of view (FoV) of the HCOPAR.
- Still in their growth phase.

Type 2 echoes

- Generated outside of the FoV of the radar, then drifted into the radar Fov.
- Most of them were in decay phase.

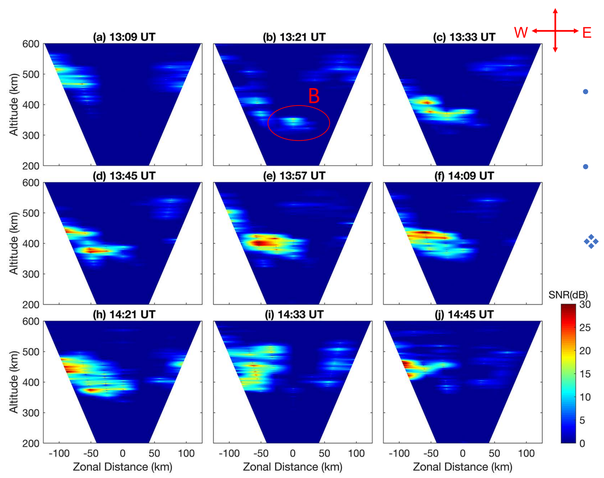

Fan sector maps

- The initiation of Group B of FAIs can be seen in (b) near 300km.
- Obvious **westward movement** of the FAIs echoes.
- The westward zonal drift of the FAIs are consistent with the zonal drift of the background plasma observed by Hainan Digisonde.

Figure 5. (a–j) Fan sector maps of the backscattered echo SNR in the zonal-vertical plane between 13:09 and 14:45 UT on 8 Sep 2017 showing the freshly generated type of the FAIs.

4 Discussion and Conclusions

Postsunset FAIs: storm-induced PPEF effect

I. Right after the second large sudden southward turning of IMF Bz, h'F at Fuke started ascending rapidly and reached to a peak altitude of ~387 km, which was **remarkably higher compared to its typical quiet day enhancement** during postsunset hours on 7 Sep 2017.

II. The F region FAIs started to emerge just a few minutes later than the time of peak uplift of h'F at Fuke. The substantial upward movement of F layer generated favorable conditions for the growth of the RT instability, which is believed to play an important role in inducing low-latitude plasma irregularities.

✓ Therefore, we conclude that the **strong eastward IEF penetrated to low-latitude ionosphere, uplifted the F layer to higher altitudes and triggered the postsunset FAIs.**

Postmidnight FAIs: substorm-related overshielding PPEF

- Under quiet condition, the ambient zonal electric field is usually westward in the postmidnight period and can cause downward plasma drift, so it does not support the FAIs generation after local midnight.
- In this case, both the uplift of F layer and irregularities occurred after midnight when the southward IMF Bz gradually recovered to its quiet time values.

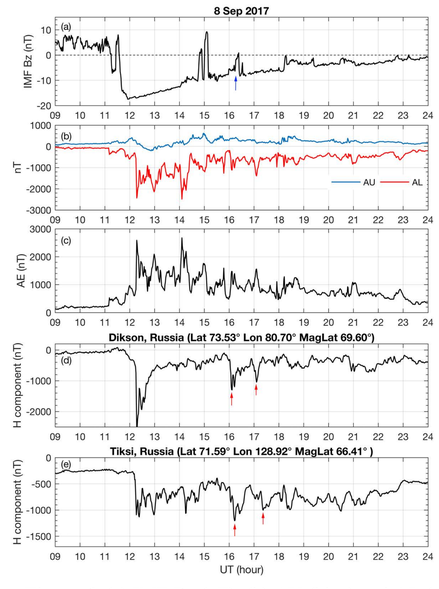

Figure 6. (a) IMF Bz (nT), (b) AU (blue) and AL (red) indices (nT), (c) AE index (nT), (d) H component (nT) at Dikson, Russia (73.53°N, 80.70°E, MagLat 69.06°N), (e) H component (nT) at Tiksi, Russia (71.59°N, 128.92°E, MagLat 66.41°N).

- Undershielding PPEF has eastward (westward) polarity on the dayside (nightside) and overshielding PPEF has opposite polarity. Therefore, eastward overshielding PPEF could be responsible for the uplift of F layer and subsequent irregularities in the postmidnight sector in this case.
- Two sharp decreases of H component at auroral latitudes between 16:00 and 18:00 UT suggested two consecutive substorm onsets while the IMF Bz was gradually recovering toward quiet time values.
- The overshielding electric field can be quickly established after a substorm onset even without the IMF Bz northward turning.
- Therefore, the large uplift of F layer and postmidnight FAIs after 17:00 UT is highly likely resulted from **substorm-related overshielding PPEF, which has eastward polarity on the night side**.

5 Future Work

The FAIs observed by the HCOPAR represented little or even no zonal drift at the beginning of the observation as shown in Figures 4d–4g. Subsequently, the irregularities traveled westward, moving together with the ambient plasma. In contrast, the quiet time zonal drift of FAIs are usually eastward. Therefore, the irregularities zonal motion pattern described above can be attributed to the reversal of the background plasma zonal drift. Further studies are required to be conducted in terms of the storm time thermospheric disturbance winds effects in future work.

This work has been accepted by Space Weather and detailed discussions can be referred to https://doi.org/10.1029/2018SW001865.